Molecular Cell, Volume *39*

A Dual E3 Mechanism for Rub1 Ligation to Cdc53

Daniel C. Scott, Julie K. Monda, Christy R.R. Grace, David M. Duda, Richard W. Kriwacki, Thimo Kurz, and Brenda A. Schulman

Item

A.

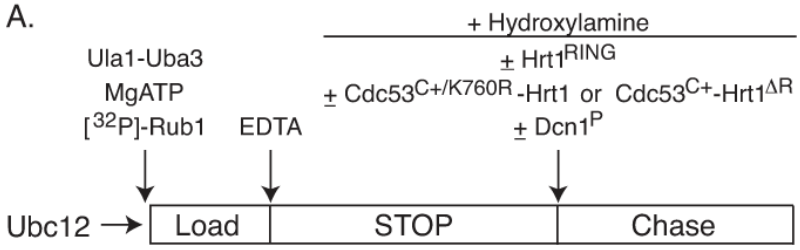

Pulse-Chase Hydroxylamine Ubc12~Rub1 discharge assay

B.

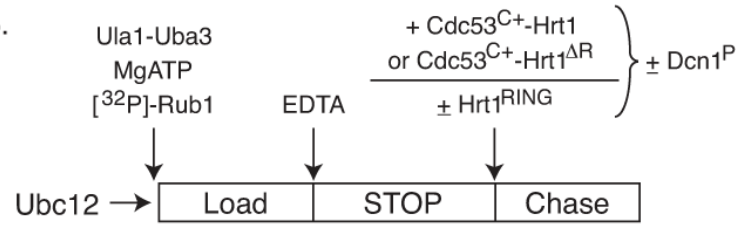

Pulse-Chase Rub1 transfer from Ubc12 to Cdc53 K760 assay

C.

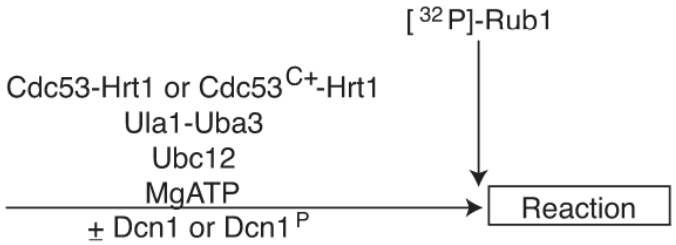

Multiple-turnover assay for Rub1 modification of Cdc53

D.

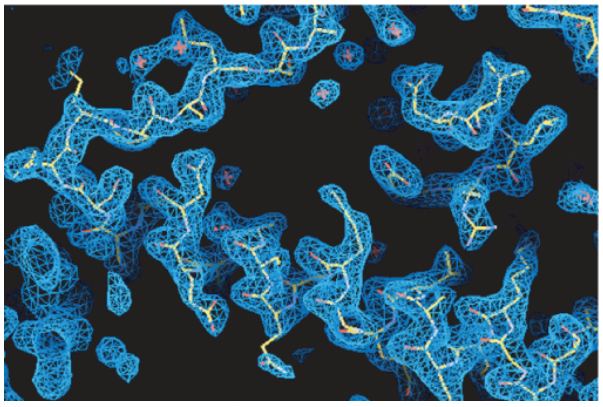

E.

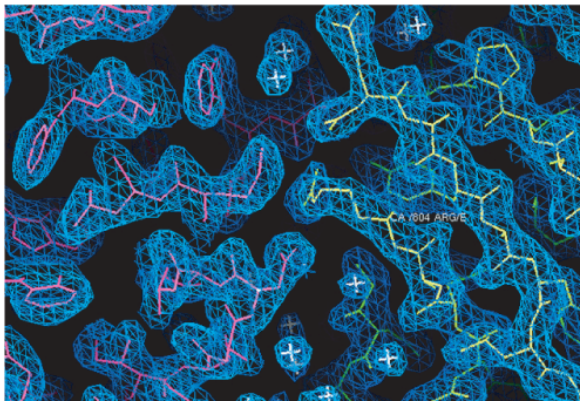

Figure S1. Experimental information.

A. Schematic view of assay for Ubc12~Rub1 discharge to hydroxylamine. Hydroxylamine serves as a nonspecific primary amine that can collide with an E2~UBL conjugate, to discharge the thioester-linked E2~UBL conjugate and produce free E2 and isopeptide-linked UBL~NHOH. Using Ula1-Uba3 (Rub1 E1) and MgATP, Ubc12 was loaded with [^{32}P]-Rub1 to form a thioester-linked Ubc12~[^{32}P]-Rub1 conjugate. This loading reaction was quenched with EDTA. Hydroxylamine was added, and Ubc12~[^{32}P]-Rub1 discharge was examined at different times by disappearance of the thioester-linked Ubc12~[^{32}P]-Rub1 conjugate, in absence or presence of the isolated Hrt1 RING domain (Hrt1^{RING}), Dcn1^{P}, or Hrt1 in complex with Cdc53$^{C+/K760R}$ in which a Lys760Arg substitution prevents Rub1 modification of Cdc53 or an Hrt1 mutant lacking the RING (ΔR) in complex with Cdc53^{C+}.

B. Schematic view of pulse-chase assay for Rub1 transfer from Ubc12 to Cdc53^{C+}. In the "pulse", Ubc12 was loaded with [^{32}P]-Rub1 by Ula1-Uba3 (Rub1 E1) in the presence of MgATP, and formation of the thioester-linked Ubc12~[^{32}P]-Rub1 conjugate was quenched with EDTA. Cdc53^{C+}-Hrt1 or a mutant lacking the Hrt1 RING domain was added, and Rub1 was "chased" from Ubc12 to Cdc53^{C+} in the absence or presence of other factors.

C. Schematic view of multiple turnover assay for generation of Rub1~Cdc53. Ula1-Uba3 (Rub1 E1), Ubc12, and various mutants of Cdc53-Hrt1 and/or Dcn1 were mixed in the presence of MgATP. Reactions were initiated by the addition of [^{32}P]-Rub1. Formation of [^{32}P]-Rub1~Cdc53 was detected at various reaction times.

D. Final $2F_o$-F_c electron density contoured at 1σ displayed over the N-terminal helix of Chain A of Ubc12.

E. Final $2F_o$-F_c electron density contoured at 1σ at the interface of Dcn1^{P} (violet) and Cdc53^{WHB} (yellow).

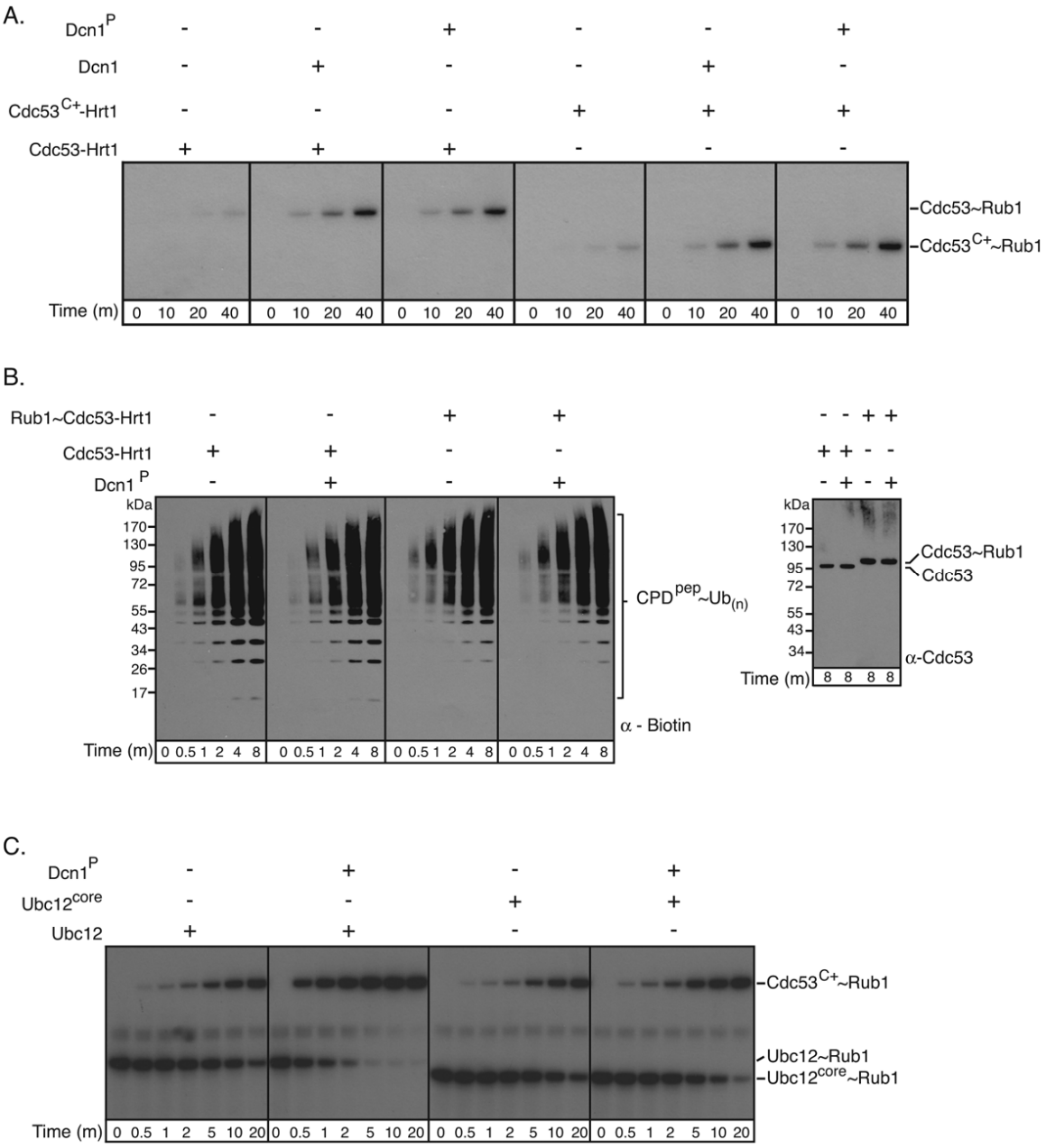
A.
Dcn1P - - + - - +
Dcn1 - + - - + -
Cdc53C+-Hrt1 - - - + + +
Cdc53-Hrt1 + + + - - -
Cdc53~Rub1
Cdc53C+~Rub1
Time (m) 0 10 20 40 0 10 20 40 0 10 20 40 0 10 20 40 0 10 20 40 0 10 20 40
B.
Rub1~Cdc53-Hrt1 - - + +
Cdc53-Hrt1 + + - -
Dcn1 P - + - +
kDa
170
130
95
72
55
43
34
26
17
CPDpep~Ub(n)
α - Biotin
Time (m) 0 0.5 1 2 4 8 0 0.5 1 2 4 8 0 0.5 1 2 4 8 0 0.5 1 2 4 8
- - + +
+ + - -
- + - +
kDa
170
130
95
72
55
43
34
Cdc53~Rub1
Cdc53
α-Cdc53
Time (m) 8 8 8 8
C.
Dcn1P - + - +
Ubc12core - - + +
Ubc12 + + - -
Cdc53C+~Rub1
Ubc12~Rub1
Ubc12core~Rub1
Time (m) 0 0.5 1 2 5 10 20 0 0.5 1 2 5 10 20 0 0.5 1 2 5 10 20 0 0.5 1 2 5 10 20

Figure S2. Dcn1 is a specific Rub1 E3 for Cdc53.
A. Phosphorimager data for multiple-turnover assay monitoring [^{32}P]-Rub1 ligation to either full-length Cdc53-Hrt1 purified from insect cells or Cdc53^{C+}-Hrt1 purified from *E. coli*, via Ula1-Uba3, Ubc12, MgATP, and in the absence or presence of Dcn1 or Dcn1^{P}.

B. Western blots monitoring SCF (i.e., Cdc53-Hrt1 based ubiquitin E3) mediated polyubiquitination in the absence or presence of Dcn1^{P}. Left panel - Anti-biotin western blot of reactions for SCF^{Cdc4}/Cdc34-mediated polyubiquitination of a biotinylated version of the high affinity Cdc4-phosphodegron (CPD) peptide. Reactions were carried out in the absence or presence of Dcn1^{P}, with either Cdc53-Hrt1 or Rub1~Cdc53-Hrt1 as indicated. Right panel - Anti-Cdc53 western blots verifying the status of Cdc53 at the end of the ubiquitination reactions.

C. Autoradiogram of long time-courses showing [^{32}P]-Rub1 transfer from Ubc12 or Ubc12^{core} to Cdc53^{C+}-Hrt1 in the absence or presence of Dcn1^{P}.

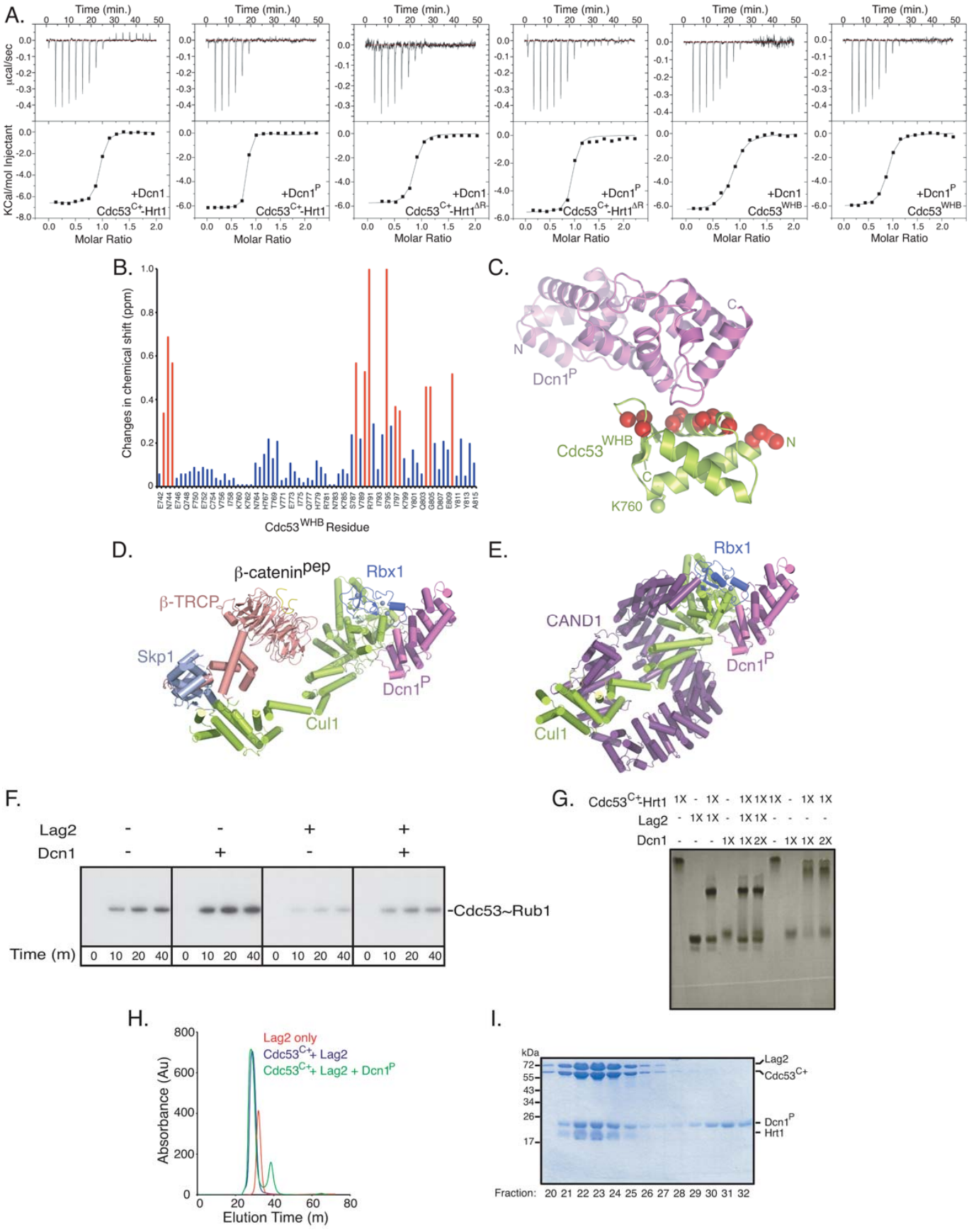
A.
Time (min.)
µcal/sec
KCal/mol Injectant
Molar Ratio
+Dcn1
Cdc53C+-Hrt1
+Dcn1P
Cdc53C+-Hrt1
+Dcn1
Cdc53C+-Hrt1ΔR
+Dcn1P
Cdc53C+-Hrt1ΔR
+Dcn1
Cdc53WHB
+Dcn1P
Cdc53WHB
B.
Changes in chemical shift (ppm)
Cdc53WHB Residue
C.
N
C
Dcn1P
Cdc53WHB
K760
D.
β-catenin pep
Rbx1
β-TRCP
Skp1
Dcn1P
Cul1
E.
Rbx1
CAND1
Dcn1P
Cul1
F.
Lag2
Dcn1
-Cdc53~Rub1
Time (m)
G.
Cdc53C+Hrt1
Lag2
Dcn1
H.
Lag2 only
Cdc53C+ Lag2
Cdc53C+ Lag2 + Dcn1P
Absorbance (Au)
Elution Time (m)
I.
kDa
Lag2
Cdc53C+
Dcn1P
Hrt1
Fraction:

Figure S3. Cdc53 interactions.
A. ITC data for binding between the indicated Cdc53-Hrt1 variants and Dcn1 variants. Upper panels – raw power data recorded during the titration experiments. Lower panels – fit of standard binding equations after integration of the raw data, using software provided by Microcal.

B. Changes in ^{1}H chemical shift for $Cdc53^{WHB}$ upon forming a 1:1 complex with $Dcn1^{P}$. Bars in red indicate residues for which ^{1}H chemical shift perturbations upon complex formation were >0.3 ppm.

C. Structure of $Dcn1^{P}$ (violet)-$Cdc53^{WHB}$ (lime), with residues highlighted as red spheres for which ^{1}H chemical shift perturbations upon complex formation were >0.3 ppm. The location of the Rub1 acceptor Lys760 is indicated in sticks, with a sphere for the ε-amino group.

D. Structural model of $Dcn1^{P}$ (violet)-Cul1 (lime)-Rbx1 (blue)-Skp1 (light blue)-βTRCP (peach)-βcatenin phosphodegron peptide (yellow). $Dcn1^{P}$ was modeled by superimposing the $Dcn1^{P}$-$Cdc53^{WHB}$ structure with the WHB subdomain of Cul1 in complex with Rbx1, Skp1, and Fbox (1LDK.pdb) (Zheng et al., 2002). Skp1-βTRCP-β-catenin phosphodegron peptide was modeled by superimposing on the Skp1-Fbox (Wu et al., 2003).

E. Structural model of $Dcn1^{P}$ (violet)-Cul1 (lime)-Rbx1 (blue)-CAND1 (purple). $Dcn1^{P}$ was modeled by superimposing the $Dcn1^{P}$-$Cdc53^{WHB}$ structure with the WHB subdomain of Cul1 in complex with Rbx1 and CAND1 (Goldenberg et al., 2004).

F. Phosphorimager data from multiple-turnover assays probing the affects of $Dcn1^{P}$ on Lag2 mediated inhibition of Rub1 modification of Cdc53-Hrt1.

G. Coomassie-stained nondenaturing polyacrylamide gel showing formation of a $Cdc53^{C+}$-Hrt1-Lag2-$Dcn1^{P}$ multiprotein complex. 8 μM $Cdc53^{C+}$-Hrt1 was incubated with 8 μM Lag2 (1X) in the absence or presence of 8 μM (1X) or 16 μM (2X) $Dcn1^{P}$ in 25 mM HEPES, 100 mM NaCl, 1 mm DTT, pH 7.5 on ice for 30 minutes. Samples were loaded onto a 4% nondenaturing gel and separated for 90 minutes at 130 V and 4°C.

H. UV traces of elution profiles analyzing $Cdc53^{C+}$-Hrt1-Lag2-$Dcn1^{P}$ complex formation by gel filtration chromatography. 50 μM Lag2 was incubated on ice for 30 minutes in 25 mM Tris, 100 mM NaCl, 1 mM DTT, pH 7.6 alone, as a mixture with 50 μM $Cdc53^{C+}$-Hrt1, or as a mixture with 50 μM $Cdc53^{C+}$-Hrt1 and 75 μM $Dcn1^{P}$. Mixtures were separated on an SD200 (GE) sizing column.

I. Coomassie-stained SDS-PAGE gel of fractions from the gel filtration separation of the 1:1:1.5 mixture of Lag2:$Cdc53^{C+}$-Hrt1:$Dcn1^{P}$.

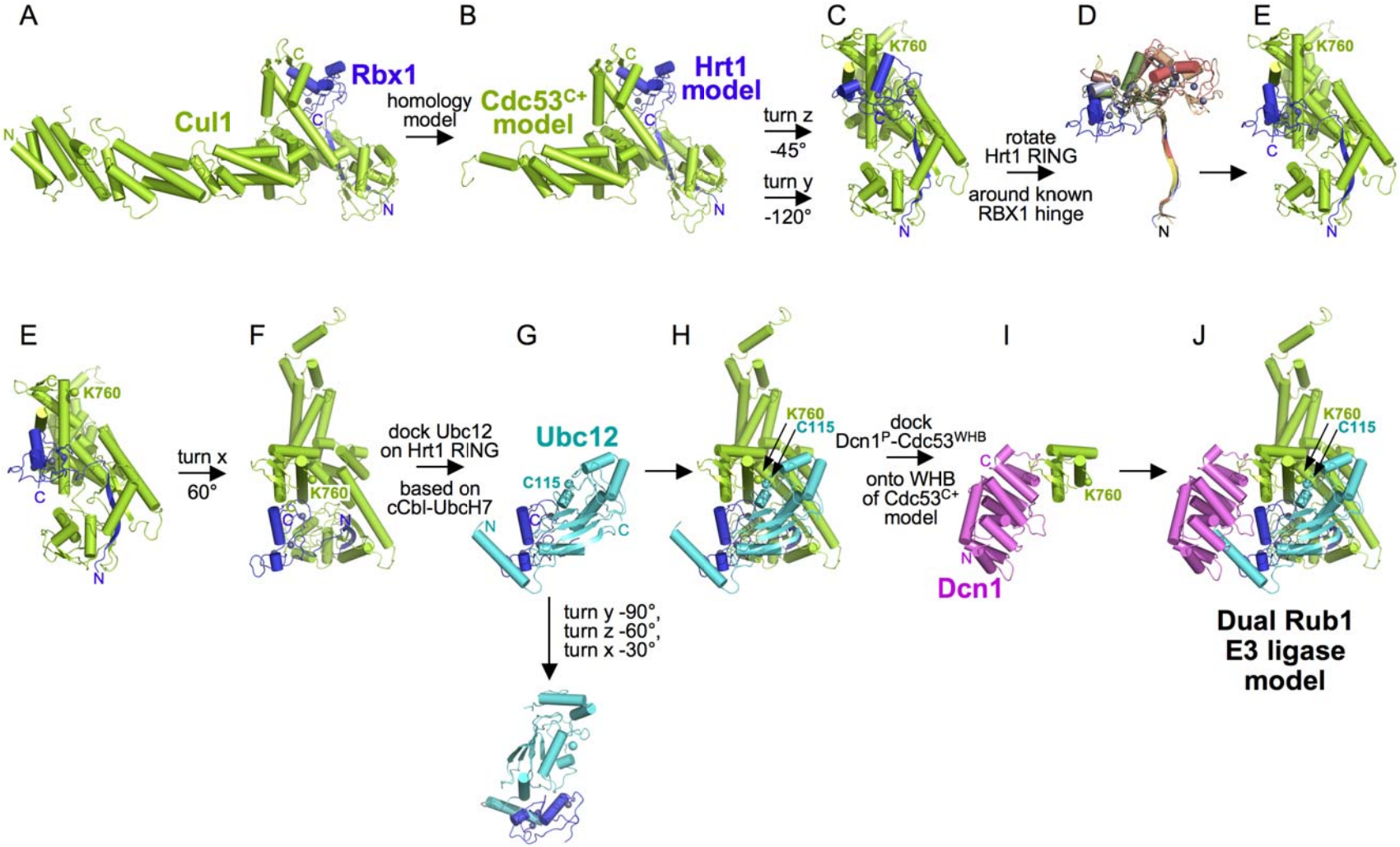
A
Cul1
Rbx1
homology model
B
Cdc53C+ model
Hrt1 model
turn z -45°
turn y -120°
C
K760
rotate Hrt1 RING
around known RBX1 hinge
D
E
K760
E
K760
turn x 60°
F
K760
dock Ubc12 on Hrt1 RING
based on cCbl-UbcH7
G
Ubc12
C115
turn y -90°, turn z -60°, turn x -30°
H
K760
C115
dock Dcn1P-Cdc53WHB
onto WHB of Cdc53C+ model
I
K760
Dcn1
J
K760
C115
Dual Rub1 E3 ligase model

Figure S4. Generation of a structural model for Dcn1^{P}-Cdc53-Hrt1-Ubc12 in a catalytic orientation. The model for Cdc53-Hrt1, obtained from the Swissmodel repository, superimposes on Cul1-Rbx1 (Zheng et al., 2002). Ubc12's core domain was docked onto the Hrt1 RING as described in Fig. 1F. We generated a catalytic model based on previous studies of human Rbx1, which showed that the hinge connecting the N-terminal cullin-binding strand and C-terminal RING is flexible (Angers et al., 2006; Duda et al., 2008; Goldenberg et al., 2004; Zheng et al., 2002), and that rotation about this hinge is important for NEDD8 transfer to human cullins (Duda et al., 2008). Rotation about the corresponding Hrt1 hinge allows positioning of the Hrt1 RING-Ubc12 such that Ubc12's catalytic Cys approaches Cdc53's Lys760. A complex with Dcn1^{P} was modeled by docking our Dcn1^{P}-Cdc53^{WHB} structure onto the Cdc53 WHB subdomain. Visualization of the steps in modeling, and orienting the model in Fig. 4D are as follows.

A. Canonical view of Cul1 (lime)-Rbx1 (blue) (1LDJ.pdb) (Zheng et al., 2002). The zinc ligands in the RING domain are grey spheres. The location of the NEDD8/Rub1 acceptor Lys is indicated in sticks, with a sphere for the ε-amino group.

B. Model of Cdc53^{C+}-Hrt1 (Swissmodel) based on the Cul1-Rbx1 structure, shown in the same orientation as Cul1-Rbx1 in (A).

C. Same as (B), but reoriented by turning -45° in z and -120° in y. In this and the following panels, the location of the Rub1 acceptor Lys760 is highlighted, with a sphere for the ε-amino group.

D. Superposition of Rbx1 structures over their N-terminal strands: 1LDJ (light blue) (Zheng et al., 2002), 1U6G (light green) (Goldenberg et al., 2004), 2HYE (yellow) (Angers et al., 2006), 3DPL.pdb (pink) and 3DQV (tan and rose) (Duda et al., 2008). The structurally-observed hinge was used as the site of rotation for the Hrt1 RING domain from that of 1LDJ.pdb as in (C) to that shown in blue.

E. Cdc53^{C+}-Hrt1 with the RING modeled in a catalytic position, obtained by rotation around the hinge structurally observed in Rbx1 as shown in (D).

F. Same as E, but reoriented by turning 60° in x.

G. Ubc12 was docked onto the Hrt1 RING based on alignment with the c-Cbl-UbcH7 structure (Zheng et al., 2000). The docking model is shown below in a canonical view for an E2-RING complex, obtained by turning the complex -90° in y, -60° in z, and -30° in x.

H. Same as F, with Ubc12 docked onto Hrt1 as in (G).

I. Structure of Cdc53^{WHB}-Dcn1^{P}.

J. Dual Rub1 E3 ligase (Dcn1^{P} and Hrt1 model), after Cdc53^{WHB}-Dcn1^{P} was superimposed on the WHB subdomain of Cdc53^{C+}-Hrt1-Ubc12 from (H). For simplification, Rub1, which would start thioester bound to Ubc12 C115 and end ligated via an isopeptide bond to Cdc53 K760, is not shown.

Table S1: Chemical Shift values for ^{1}H and ^{15}N resonances (in ppm) for $Cdc53^{WHB}$ in the absence and presence of $Dcn1^{P}$.

Residues	$Cdc53^{WHB}$ alone		$Cdc53^{WHB}$ -$Dcn1^{P}$ Complex	
	^{1}H	^{15}N	^{1}H	^{15}N
E742	8.81	123.60	8.75	123.57
L743	8.15	122.66	8.23	123.39
N744	8.27	119.32	8.35	120.84
T745	8.10	116.86	8.23	118.09
E746	8.19	121.49	8.18	121.41
R747	8.06	119.79	8.01	119.85
Q748	7.88	118.32	7.9	118.2
I749	8.01	119.44	8.07	119.52
F750	7.76	121.25	7.71	121.09
L751	8.49	120.14	8.53	120.25
E752	8.60	118.26	8.62	118.46
A753	7.70	120.14	7.66	119.98
C754	7.95	118.97	8.01	119.08
I755	8.09	119.02	8.11	118.95
V756	8.10	119.20	8.12	119.24
R757	7.59	118.56	7.63	118.66
I758	7.96	119.79	7.96	119.86
M759	8.57	116.27	8.61	116.28
K760	8.60	122.05	8.59	122.02
A761	6.64	117.50	6.65	117.49
K762	8.20	115.22	8.21	115.23
R763	8.51	114.98	8.51	115
N764	8.78	120.67	8.77	120.91
L765	8.49	123.48	8.58	123.44
H767	8.64	123.83	8.61	123.5
T768	8.89	111.99	8.81	112.46
T769	6.69	115.69	6.68	115.4
L770	8.09	121.84	7.97	121.46
V771	8.25	117.80	8.28	117.81

Residues	$Cdc53^{WHB}$ alone		$Cdc53^{WHB}$ -$Dcn1^{P}$ Complex	
	^{1}H	^{15}N	^{1}H	^{15}N
N772	7.93	116.51	7.96	116.49
E773	8.57	121.98	8.46	121.97
C774	8.38	119.49	8.43	119.57
I775	8.32	121.25	8.36	121.21
A776	7.95	122.19	7.93	122.18
Q777	8.12	114.92	8.14	114.99
S778	7.86	112.93	7.87	113
H779	7.45	120.61	7.42	120.35
Q780	8.20	117.21	8.18	117.01
R781	8.09	118.03	8.06	117.91
F782	7.75	113.87	7.75	113.86
N783	8.53	118.15	8.54	118.13
A784	8.00	126.59	8.03	126.7
K785	7.62	120.70	7.54	120.68
V786	8.94	123.54	9	123.56
S787	8.57	113.58	8.6	114.1
M788	7.11	121.60	6.97	120.36
V789	7.61	120.78	7.58	120.3
K790	8.64	118.97	8.93	117.98
R791	7.32	117.56	7.63	119.68
A792	7.43	123.01	7.32	123.6
I793	8.23	119.44	8.31	119.39
D794	8.30	118.85	8.16	118.42
S795	7.98	116.04	7.84	113.69
L796	7.83	119.85	7.91	119.25
I797	8.42	122.37	8.6	123.08
Q798	8.09	122.78	8.41	122.43
K799	8.06	115.33	8.19	115.41
G800	7.65	105.84	7.65	105.75
Y801	8.03	115.98	7.99	116.36
L802	6.78	114.92	6.86	115.1

Residues	$Cdc53^{WHB}$ alone		$Cdc53^{WHB}$ -$Dcn1^{P}$ Complex	
	^{1}H	^{15}N	^{1}H	^{15}N
Q803	8.78	119.08	8.83	119.03
R804	9.16	126.12	9.37	127.03
G805	8.44	112.52	8.52	113.52
D806	8.69	122.25	8.77	122.66
D807	8.02	115.83	8.09	115.78
G808	7.91	107.36	7.81	106.96
E809	8.00	118.21	7.84	118.11
S810	7.40	113.75	7.04	112.92
Y811	8.59	116.34	8.62	116.41
A812	8.83	122.19	9.01	122.46
Y813	8.57	122.07	8.53	122.03
L814	7.77	128.40	7.79	128.84
A815	6.26	128.05	6.36	128.13

SUPPLEMENTAL EXPERIMENTAL PROCEDURES

Constructs, Protein preparation, and Antibodies

All proteins are from yeast, except the human UbcH5b and ubiquitin E1 (UBA1) used in Fig. S2 and 5, which were prepared as described (Huang et al., 2009). Expression constructs were generated by standard molecular techniques, with coding sequences entirely verified. Mutant versions of proteins used in this study were generated by QuickChange (Stratagene). UbcH5b, Lag2, Ula1-Uba3, Ubc12, Dcn1, $Dcn1^{P}$, Skp1-$Cdc4^{\Delta D\text{-domain}}$, and Rub1 were prepared as described (Siergiejuk et al., 2009). $Ubc12^{core}$ corresponds to residues 25 to the C-terminal 188; $Cdc53^{WHB}$ used in all experiments except Crystal Form 1 corresponds to Cdc53 residues 742 to the C-terminal residue 815, $Cdc53^{WHB}$ used only in crystal form 1 corresponds to Cdc53 residues 726 to the C-terminal residue 815; $Hrt1^{RING}$ corresponds to Hrt1 residues 49 the C-terminal residue 121; $Hrt1^{\Delta R}$ lacks residues 49-121; Ubc12N-UbcH5b corresponds to residues 1-24 of Ubc12 fused at the N-terminus of UbcH5b; and $Ubc12^{C115only}$ contains Ala substitutions in place of Cys99 and Cys158. These and Cdc34 were expressed as GST fusions in *E. coli* and purified by glutathione affinity chromatography. After TEV protease treatment proteins were further purified by ion-exchange and gel filtration chromatography in 25mM Tris, 125mM NaCl, 5mM DTT, pH 7.6, concentrated (Amicon Ultra), aliquotted, flash-frozen, and stored at -80 °C. Constructs for purification of $Cdc53^{C+}$-Hrt1 (endogenously truncated upon expression of Cdc53-Hrt1 in bacteria) and baculoviruses for purification of full-length Cdc53-Hrt1 from insect cells were described previously (Siergiejuk et al., 2009).

Antibodies against Cdc53 (sc-50444) and Ubc12 (sc-8935) were obtained from Santa Cruz Biotechnology, and against Biotin (100-4198) were from Rockland, and used according to the manufacturers' instructions. Peptides were synthesized and purified by reversed-phase HPLC by the Hartwell Center for Bioinformatics and Biotechnology at St. Jude. The SCF^{Cdc4} ubiquitination substrate peptide corresponds to the high affinity Cdc4 phosphodegron sequence (Orlicky et al., 2003), with the substrate peptide sequence (KAMLSEQNRASPLPSGLLT*PPQS*GRRASY, *=phosphorylation) described previously (Pierce et al., 2009), including the N-terminal acetylation, except with the C-terminal His-tag replaced by a biotin. The $Ubc12^{N}$ peptide corresponds to residues 1-24, and has the sequence MLKLRQLQKKKQKENENSSSIQPN, with amidation of the C-terminus.

Isothermal Titration Calorimetry

Protein samples were buffer matched by desalting over a NAP-5 column (GE) into 25 mM MES, 100 mM NaCl, 1 mM BME, pH 6.7. Measurements were performed on a MicroCal ITC200. Cdc53-Hrt1 and variants thereof were placed into the sample cell at a final concentration of 25 μM at 22°C. The ligands Dcn1 or $Dcn1^{P}$ were constantly injected (2.5 μl). The interval time between each injection was 3 minutes and the duration of each injection was 5 seconds. Obtained spectra were evaluated using Origin (V 7.0) to determine heats of binding and K_d values.

Crystallography

Crystals were grown by the hanging-drop vapor-diffusion method. All reflection data were processed with HKL2000 (Otwinowski and Minor, 1997).

Crystals of Ubc12 were grown at room temperature in 27% PEG3350, 0.1 M Tris, 0.2 M NaCl, pH 7.6. The crystals were soaked in well solution supplemented with 25% glycerol prior to flash-freezing in liquid nitrogen. Reflection data were collected at 22-BM SERCAT at the Advanced Photon Source. The crystals belong to space group $P2_12_12_1$

with two molecules in the asymmetric unit. Phases were obtained by molecular replacement with PHASER (Storoni et al., 2004), using two copies of human $Ubc12^{core}$ (Huang et al., 2005). The structure was built using COOT (Emsley and Cowtan, 2004), and refined with PHENIX (Adams et al., 2010). The final structure contains all residues for Chain A, including two at the N-terminus from cloning, from residues 2 to the C-terminal 188 in Chain B.

Crystals of $Cdc53^{WHB}$-$Dcn1^{P}$ (form 1) were grown at 4°C in 27% PEG3000, 0.1M Tris, 0.2 M lithium sulfate, pH 8.0, and of form 2 were grown at room temperature in 21% PEG3350, 0.1 M Bis-Tris-Propane, 0.2 M sodium fluoride, pH 7.9. Crystals were flash-frozen in liquid nitrogen after harvesting from mother liquor supplemented with 30% glycerol. Poorly-diffracting crystals were initially obtained for Form 2, with data to ~3.9 Å resolution collected at the ALS 8.2.1 beamline. An initial structure was determined by molecular replacement using PHASER (Storoni et al., 2004) searching with 4 copies of $Dcn1^{P}$ and 2 copies of a model for $Cdc53^{WHB}$ generated by Modeller (Eswar et al., 2006). Another 2 copies of the model for $Cdc53^{WHB}$ were placed into clear density based on noncrystallographic symmetry for the two complexes. However, refinement was challenging, due to low resolution and weak data. Better data for form 2 were collected at the 24-ID-C NECAT beamline, as well as obtaining data for the other crystal form 1. Although crystal form 1 yielded far superior diffraction, to better than 2 Å resolution, these were small crystals grown together, in such a way as to preclude their separation. We were unable to take full advantage of the diffraction due to the numerous lattices. To obtain useable data and separate the numerous lattices, it was necessary to use a microbeam (24-ID-E, NECAT) and move the detector out and cut the data off at 2.23 Å resolution. The final model contains $Cdc53^{WHB}$ residues 730 to the C-terminus, and $Dcn1^{P}$ residues 71 to the C-terminus. The structure of form 1 was obtained by molecular replacement using PHASER, by searching for one copy of the $Cdc53^{WHB}$-$Dcn1^{P}$ complex from the original solution to form 2. After autobuilding with PHENIX, the additional residues were built manually in O (Jones et al., 1991), with subsequent refinement using PHENIX performed with alternating cycles of building using COOT (Emsley and Cowtan, 2004). The high-resolution structure of form 1 was ultimately used as the model to search the new data for form 2. 4 copies were found with PHASER, with a 5^{th} placed manually into weak electron density that persisted throughout refinement but remained low quality. Accordingly, the 5^{th} copy of the complex has higher B-factors. The structure was refined with CNS (Brunger et al., 1998).

Biochemical assays

Ligation of Rub1 to Cdc53 under multiple turnover conditions was assayed with 8 nM Ula1-Uba3, 80 nM Cdc53-Hrt1 or $Cdc53^{C+}$-Hrt1, 80 nM Ubc12, +/- 80 nM Dcn1 (or $Dcn1^{P}$) in 50 mM Tris, 100 mM NaCl, 1.25 mM ATP, 2.5 mM $MgCl_2$, pH 7.6. Reactions were carried out at 18 °C (the ambient room temperature of our room dedicated for radioactive work) and initiated by the addition of 1 μM [^{32}P]-Rub1. Aliquots were removed at the indicated times and quenched in 2X SDS-sample buffer.

For pulse-chase type assays, 10 μM wild-type and indicated mutant versions of Ubc12 were loaded for 40 minutes at 30 °C with 0.8 μM Ula1-Uba3, 15 μM [^{32}P]-Rub1, in 50 mM Hepes, 100 mM NaCl, 1.25 mM ATP, 2.5 mM $MgCl_2$, pH 7.5. After 40 minutes, formation of Ubc12~Rub1 was quenched with 50 mM EDTA at room temperature for 5 minutes. For the chase reactions, 40 nM Ubc12~[^{32}P]-Rub1 thioester conjugate was diluted into 50 mM Bis-Tris, 100 mM NaCl, 50 mM EDTA, 0.5 mg/ml BSA, pH 6.8. Chase reactions were initiated at 18 °C by the addition of $Cdc53^{C+}$-Hrt1 or Dcn1-

$Cdc53^{C+}$-Hrt1 at a final concentration of 0.5 μM. For Ubc12~[^{32}P]-Rub1 discharge to hydroxylamine, chase mixes were prepared containing 20 μM $Hrt1^{RING}$, $Cdc53^{C+/K760R}$-Hrt1, $Cdc53^{C+/K760R}$-$Hrt1^{\Delta R}$, or $Cdc53^{C+/K760R}$-Hrt1 ± 20 μM $Dcn1^{P}$ in 50 mM Bis-Tris, 100 mM NaCl, 50 mM EDTA, 10 mM Hydroxylamine, pH 7.8; [^{32}P]-Rub1 discharge initiated by the addition of Ubc12~[^{32}P]-Rub1 thioester conjugate to a final concentration of 40 nM. $Ubc12^{N}$ inhibition was tested with addition of 0.5 mM peptide. Aliquots were removed at the indicated times and quenched with 2X SDS-PAGE sample buffer. Reaction products were heated at 70°C for 1.5 minutes and separated on 4-12% NuPAGE gels (Invitrogen). Dried gels were exposed to a Storm (GE) Phosphoimager screen and the amount of $Cdc53^{C+}$~[^{32}P]-Rub1 formed quantified as arbitrary units with ImageQuant (GE). Discharge assays were normalized by setting the amount of Ubc12~[^{32}P]-Rub1 (wild-type or mutant versions) at the first time-point to 100% and results presented as the % of Ubc12~[^{32}P]-Rub1 remaining at each time-point of the assay. Chase reactions were normalized by setting the amount of $Cdc53^{C+}$~[^{32}P]-Rub1 formed at the last time point to 100%. In cases where wild-type and mutant versions of Ubc12 were compared, the amount of $Cdc53^{C+}$~[^{32}P]-Rub1 formed at each point of the chase was corrected prior to normalization to represent the amount of $Cdc53^{C+}$~[^{32}P]-Rub1 formed per amount of Ubc12~[^{32}P]-Rub1 thioester present at time zero of the chase.

For kinetic measurements, pulse formation of a Ubc12 (Asn107Ala)~[^{32}P]-Rub1 conjugate and EDTA quenching was as described above. 40 nM Ubc12~Rub1 was diluted into chase mixes containing 50 mM Bis-Tris, 100 mM NaCl, 50 mM EDTA, 0.5 mg/ml BSA, pH 6.0. Chase reactions were initiated at 18°C by the addition of $Cdc53^{C+}$-Hrt1 ± $Dcn1^{P}$ (1:1) to a final concentration ranging from 15 μM to 700 μM. Aliquots were quenched with 2X SDS-PAGE sample buffer at four different time points for each reaction to ensure reaction rates were under initial velocity conditions. The amount of $Cdc53^{C+}$~Rub1 formed during the chase was quantified by comparison to a standard curve generated from serial dilutions of known amounts of free [^{32}P]-Rub1. Initial velocities at the various concentrations of $Cdc53^{C+}$-Hrt1 or $Dcn1^{P}$-$Cdc53^{C+}$-Hrt1 were obtained by plotting the amount of Rub1~$Cdc53^{C+}$ formed divided by the amount of Ubc12~Rub1 thioester at time zero of the chase versus time. Kinetic constants for the reactions were obtained by evaluation of the data in GraFit v 5.0 (Erathicus) using a standard Michaelis-Menten enzyme kinetics equation. Data shown are from the averages obtained from three independent experiments. The high level of $Cdc53^{C+}$-Hrt1 required for kinetic titrations required purification from >100 liters of bacterial culture to achieve three independent repetitions.

Cross-linking

All proteins used in the cross-linking studies were pre-incubated in 10 mM DTT followed by desalting into 50 mM Tris, 100 mM NaCl, pH 7.6 over Zeba desalting column (Pierce) to completely reduce free cysteines. 100 μM Ubc12 was mixed with a five-fold molar excess of Bis-Maleimidoethane (BMOE) (Pierce) and incubated on ice for 1.5 hours followed by removal of unreacted cross-linker by passage over a Zeba desalting column. Cross-linking reactions were initiated by the addition of the Ubc12~BMOE products to a final concentration of 10 μM into mixtures containing 50 mM Tris, 150 mM NaCl, 1 μM $Cdc53^{C+}$-Hrt1 (+/- 1 μM $Dcn1^{P}$), pH 7.6 at room temperature. At the indicated times, aliquots of the cross-linking reactions were removed and quenched on ice for 15 minutes in buffer containing 50 mM DTT. Samples were subsequently quenched with 2X SDS-PAGE sample buffer containing 10 mM DTT and separated on

4-12% Nu-PAGE gels (Invitrogen). After western transfer, nitrocellulose membranes were probed with anti-Cdc53 or anti-Ubc12 antibodies. After scale-up and purification of the cross-linked Hrt1-Cdc53$^{C+/K760C}$~Ubc12^{C115only}-Dcn1^{P} complex and tryptic digestion, mass spectrometry performed by the Hartwell Center for Bioinformatics and Biotechnology at St. Jude confirmed identification of the BMOE-cross-linked peptides as expected, having sequences GNVC*NLILR and IMC*AK corresponding to Cys115 and Cys760 from Ubc12^{C115only} and Cdc53$^{C+/K760C}$, respectively, with no evidence of Ubc12 crosslinking to any other peptides from Cdc53.

Ubiquitination of CPD peptide

5 μM Cdc53-Hrt1 was modified with Rub1 by incubation with 0.9 μM Ula1-Uba3, 5 μM Ubc12, and 30 μM Rub1, or 0.3μM Ula1-Uba3, 1.2 μM Ubc12, 5 μM Cdc53-Hrt1, 30 μM Rub1, and 5μM Dcn1^{P} in 50 mM Tris, 100 mM NaCl, 2.5 mM $MgCl_2$, 1.25 mM ATP, pH 7.6 at room temperature for 40 or 20 minutes, respectively. Ubiquitination reactions contained 100 nM Cdc53-Hrt1 (or 100nM Rub1~Cdc53-Hrt1), 100 nM Skp1-Cdc4$^{\Delta D\text{-domain}}$, 250 nM UBA1, 300 nM Cdc34, 50 μM ubiquitin (Sigma), 5 μM biotinylated CPD peptide, +/- 100 nM Dcn1^{P} in 25 mM Tris, 40 mM NaCl, 1.25 mM ATP, 2.5 mM $MgCl_2$, pH 7.6. Reactions were initiated by the addition of ubiquitin, quenched in 2X SDS-PAGE sample buffer at the indicated times, heated at 90°C for 1.5 minutes, and separated on 4-12% NuPAGE gels. After transfer to nitrocellulose, membranes were probed with anti-biotin antibodies to detect ubiquitin conjugates. A separate aliquot of the 8 minute timepoint for each reaction was also probed with anti-Cdc53 antibodies to verify that Cdc53 itself remained either unmodified or modified by a single Rub1 during the course of the reaction.

NMR Experiments

NMR spectra were recorded on either ^{15}N-labeled or ^{15}N, ^{13}C-labeled free Cdc53^{WHB} and Cdc53^{WHB} in complex with unlabeled Dcn1^{P} at 293K using Bruker Avance 600 or 800 MHz NMR spectrometers equipped with ^{1}H/^{13}C detect, TCI triple resonance cryogenic probes. The NMR samples contained either 0.2mM ^{15}N-labeled Cdc53^{WHB} or 0.5mM ^{15}N, ^{13}C-labeled Cdc53^{WHB} in 10mM Phosphate, 100mM NaCl, 1 mM βME, 90% H_2O /10% D_2O at pH 7.0. The [^{1}H, ^{15}N] TROSY spectrum of the complex was measured on ^{15}N-labeled Cdc53^{WHB} mixed with unlabeled Dcn1^{P} in molar ratios of 1:0.25, 1:0.5, 1:0.75, 1:1 and 1:2. The NMR sample of the complex used for the backbone assignment contained equimolar concentrations of ^{15}N, ^{13}C-labeled Cdc53^{WHB} and unlabeled Dcn1^{P}. The backbone chemical shift assignments were obtained using a standard triple resonance assignment strategy through the analysis of two-dimensional [^{1}H, ^{15}N] TROSY and three-dimensional HNCA, HNCACB and CBCA(CO)NH spectra of free Cdc53^{WHB} and Cdc53^{WHB} in complex with unlabeled Dcn1^{P}. The spectra were processed using Bruker Topspin NMR software and analyzed using the computer-aided resonance software, CARA (Keller, 2003).

SUPPLEMENTAL REFERENCES

Adams, P.D., Afonine, P.V., Bunkoczi, G., Chen, V.B., Davis, I.W., Echols, N., Headd, J.J., Hung, L.W., Kapral, G.J., Grosse-Kunstleve, R.W.*, et al.* (2010). PHENIX: a comprehensive Python-based system for macromolecular structure solution. Acta Crystallogr D Biol Crystallogr *66*, 213-221.

Angers, S., Li, T., Yi, X., MacCoss, M.J., Moon, R.T., and Zheng, N. (2006). Molecular architecture and assembly of the DDB1-CUL4A ubiquitin ligase machinery. Nature *443*, 590-593.

Brunger, A.T., Adams, P.D., Clore, G.M., DeLano, W.L., Gros, P., Grosse-Kunstleve, R.W., Jiang, J.S., Kuszewski, J., Nilges, M., Pannu, N.S.*, et al.* (1998). Crystallography & NMR system: A new software suite for macromolecular structure determination. Acta Crystallogr D Biol Crystallogr *54*, 905-921.

Duda, D.M., Borg, L.A., Scott, D.C., Hunt, H.W., Hammel, M., and Schulman, B.A. (2008). Structural insights into NEDD8 activation of cullin-RING ligases: conformational control of conjugation. Cell *134*, 995-1006.

Emsley, P., and Cowtan, K. (2004). Coot: model-building tools for molecular graphics. Acta Crystallogr D Biol Crystallogr *60*, 2126-2132.

Eswar, N., Webb, B., Marti-Renom, M.A., Madhusudhan, M.S., Eramian, D., Shen, M.Y., Pieper, U., and Sali, A. (2006). Comparative protein structure modeling using Modeller. Curr Protoc Bioinformatics *Chapter 5*, Unit 5 6.

Goldenberg, S.J., Cascio, T.C., Shumway, S.D., Garbutt, K.C., Liu, J., Xiong, Y., and Zheng, N. (2004). Structure of the Cand1-Cul1-Roc1 complex reveals regulatory mechanisms for the assembly of the multisubunit cullin-dependent ubiquitin ligases. Cell *119*, 517-528.

Huang, D.T., Ayrault, O., Hunt, H.W., Taherbhoy, A.M., Duda, D.M., Scott, D.C., Borg, L.A., Neale, G., Murray, P.J., Roussel, M.F.*, et al.* (2009). E2-RING expansion of the NEDD8 cascade confers specificity to cullin modification. Mol Cell *33*, 483-495.

Huang, D.T., Paydar, A., Zhuang, M., Waddell, M.B., Holton, J.M., and Schulman, B.A. (2005). Structural basis for recruitment of Ubc12 by an E2 binding domain in NEDD8's E1. Mol Cell *17*, 341-350.

Jones, T.A., Zou, J.Y., Cowan, S.W., and Kjeldgaard, M. (1991). Improved methods for building protein models in electron density maps and the location of errors in these models. Acta Crystallogr A *47*, 110-119.

Keller, R.L.J. (2003). The computer aided resonance assignment tutorial. CANTINA, Verlag, Zurich, Switzerland.

Orlicky, S., Tang, X., Willems, A., Tyers, M., and Sicheri, F. (2003). Structural basis for phosphodependent substrate selection and orientation by the SCFCdc4 ubiquitin ligase. Cell *112*, 243-256.

Otwinowski, Z., and Minor, W. (1997). Processing of X-ray Diffraction Data Collected in Oscillation Mode. In Methods in Enzymology, Macromolecular Crystallography, part A, C.W. Carter, and R.M. Sweet, eds., pp. 307-326.

Pierce, N.W., Kleiger, G., Shan, S.O., and Deshaies, R.J. (2009). Detection of sequential polyubiquitylation on a millisecond timescale. Nature *462*, 615-619.

Siergiejuk, E., Scott, D.C., Schulman, B.A., Hofmann, K., Kurz, T., and Peter, M. (2009). Cullin neddylation and substrate-adaptors counteract SCF inhibition by the CAND1-like protein Lag2 in Saccharomyces cerevisiae. EMBO J *28*, 3845-3856.

Storoni, L.C., McCoy, A.J., and Read, R.J. (2004). Likelihood-enhanced fast rotation functions. Acta Crystallogr D Biol Crystallogr *60*, 432-438.

Wu, G., Xu, G., Schulman, B.A., Jeffrey, P.D., Harper, J.W., and Pavletich, N.P. (2003). Structure of a beta-TrCP1-Skp1-beta-catenin complex: destruction motif binding and lysine specificity of the SCF(beta-TrCP1) ubiquitin ligase. Mol Cell *11*, 1445-1456.

Zheng, N., Schulman, B.A., Song, L., Miller, J.J., Jeffrey, P.D., Wang, P., Chu, C., Koepp, D.M., Elledge, S.J., Pagano, M.*, et al.* (2002). Structure of the Cul1-Rbx1-Skp1-F boxSkp2 SCF ubiquitin ligase complex. Nature *416*, 703-709.

Zheng, N., Wang, P., Jeffrey, P.D., and Pavletich, N.P. (2000). Structure of a c-Cbl-UbcH7 complex: RING domain function in ubiquitin-protein ligases. Cell *102*, 533-539.